



Hyperfine fields in the BaFe₂As₂ family and their relation to the magnetic moment

Gerald Derondeau,^{1,*} Ján Minár,^{1,2} and Hubert Ebert¹

¹*Department Chemie, Physikalische Chemie, Universität München, Butenandtstrasse 5-13, 81377 München, Germany*

²*New Technologies Research Center, University of West Bohemia, Pilsen, Czech Republic*

(Received 29 September 2016; published 12 December 2016)

The hyperfine field B_{hf} and the magnetic properties of the BaFe₂As₂ family are studied using the fully relativistic Dirac formalism for different types of substitution. The study covers electron doped Ba(Fe_{1-x}Co_x)₂As₂ and Ba(Fe_{1-x}Ni_x)₂As₂, hole doped (Ba_{1-x}K_x)Fe₂As₂, and also isovalently doped Ba(Fe_{1-x}Ru_x)₂As₂ and BaFe₂(As_{1-x}P_x)₂ for a wide range of the concentration x . For the substituted compounds the hyperfine fields show a very strong dependence on the dopant type and its concentration x . Relativistic contributions were found to have a significantly stronger impact for the iron pnictides when compared to bulk Fe. As an important finding, we demonstrate that it is not sensible to relate the hyperfine field B_{hf} to the average magnetic moment μ of the compound, as it was done in earlier literature.

DOI: [10.1103/PhysRevB.94.214508](https://doi.org/10.1103/PhysRevB.94.214508)

I. INTRODUCTION

Since the discovery of high-temperature superconductivity in La(O_{1-x}F_x)FeAs [1,2] the iron pnictides are currently one of the most important prototype systems for unconventional superconductivity. The mechanism of superconductivity is more than likely connected to magnetic fluctuations [3–5], which makes the magnetic behavior of the iron pnictides a crucial property [6,7]. Despite tremendous research over the last years the complex magnetism of these compounds is still nontrivial to explain and some problems remain unsolved.

For example, a discrepancy is observed concerning the magnitude of the magnetic moment, depending on the chosen experimental method. Neutron diffraction data predict for the low-temperature phase of BaFe₂As₂ a total magnetic moment of 0.87 μ_B per Fe from powder samples [8], while from ⁵⁷Fe Mössbauer spectroscopy [9,10] a value between 0.4 μ_B and 0.5 μ_B was estimated. One should note that the magnetic moments in the iron pnictides are generally considered to behave nearly itinerant [4,6,11–13], although sometimes a localized picture might be more appropriate [14–16]. Furthermore, density functional theory (DFT) calculations often overestimate the magnitude of the magnetic moments, ranging from approximately 1.2 μ_B up to 2.6 μ_B [7,11,17–19]. Thus, the magnetic moments are known to be highly sensitive to the system and computational parameters, which makes estimations difficult and leads sometimes to seemingly contradicting reports [7,9,20–22]. Furthermore, the importance of spin-orbit coupling for the iron pnictides was only recently stressed [23].

Nowadays, a lot of ⁵⁷Fe Mössbauer spectroscopy data are available for the BaFe₂As₂ family with different types of substitution and doping [10,24–27]. The previously mentioned discrepancy between neutron diffraction and ⁵⁷Fe Mössbauer spectroscopy is often ascribed to possible nonzero contributions of d orbitals to the hyperfine field with an opposite sign to that of the Fermi contact field [24]. This would explain why the suggested hyperfine proportionality constant A between the experimentally measured hyperfine field B_{exp} and the

underlying magnetic moment $\mu(\text{Fe})$ has a nonlinear behavior and is in particular not comparable to the corresponding value for bulk Fe. This would imply that a more reliable estimation of magnetic moments based on ⁵⁷Fe Mössbauer spectroscopy lies not between 0.4 μ_B and 0.5 μ_B but has a higher value. Although such aspects were already suggested as a most likely explanation for this discrepancy [24], a quantitative study of the theoretical hyperfine fields including relativistic contributions is still missing [28].

To clarify this situation, we address in this paper the antiferromagnetic state of the undoped mother compound BaFe₂As₂ together with a large variety of different types of substitution. These include electron doping in the case of Ba(Fe_{1-x}Co_x)₂As₂ and Ba(Fe_{1-x}Ni_x)₂As₂, hole doping as in (Ba_{1-x}K_x)Fe₂As₂, and also isovalently doped compounds such as Ba(Fe_{1-x}Ru_x)₂As₂ and BaFe₂(As_{1-x}P_x)₂. To deal adequately with substitutional systems the fully relativistic Korringa-Kohn-Rostoker-Green's function (KKR-GF) approach is used, which was already shown to be an appropriate tool to investigate various properties of the iron pnictides [29–31]. Chemical disorder due to substitution is dealt by means of the coherent potential approximation (CPA), which effectively gives results comparable to the tedious average over many supercell configurations and is much more reliable than the virtual crystal approximation (VCA) [29,32]. Application of the CPA to the iron pnictides was already shown to be quite successful [29,30,33–35]. Using this approach, one can not only investigate the type-resolved evolution of magnetic moments with composition, but also the doping dependence of the hyperfine fields. Furthermore, all contributions to the total hyperfine field B_{hf} can be separated, revealing the direct impact of orbital non- s -electron parts within the fully relativistic approach.

II. COMPUTATIONAL DETAILS

All calculations have been performed self-consistently and fully relativistically within the four component Dirac formalism, using the Munich SPR-KKR program package [36,37]. The crystal structure is based on the orthorhombic, antiferromagnetic phase of BaFe₂As₂ in its experimentally observed stripe spin state using a 4-Fe unit cell. This implies

*gerald.derondeau@cup.uni-muenchen.de

antiferromagnetically ordered chains along the a and c axes and ferromagnetically ordered chains along the b axis. With spin-orbit coupling included within the relativistic approach the orientation of the magnetic moments was chosen to be in plane along the a axis, in line with experiment [20]. The lattice parameters and As position z were chosen according to experimental x-ray data [9]. To account for the influence of different substitutions, a linear interpolation of the lattice parameters with respect to the concentration x was performed based on Vegard's law [38]. This interpolation was individually done for each type of substitution, based on available experimental data [9,39–43]. More details on this procedure can be found in previous publications [29,30]. The treatment of disorder introduced by substitution is dealt with by means of the CPA. For the angular momentum expansion of the KKR Green's function an upper limit $\ell_{\max} = 4$ was used, i.e., s , p , d , f , and g orbitals were included in the basis set, although contributions to the hyperfine field of Fe from f and g orbitals are zero, as one would expect. All DFT calculations used the local spin-density approximation (LSDA) exchange-correlation potential with the parametrization as given by Vosko, Wilk, and Nusair [44]. The calculation and decomposition of the hyperfine field B_{hf} is done in its fully relativistic form as discussed in detail in Ref. [45].

III. RESULTS AND DISCUSSION

A. Undoped mother compound

The calculated total magnetic moment of Fe in the undoped mother compound BaFe_2As_2 is $\mu(\text{Fe}) = 0.73 \mu_{\text{B}}$, as was already published in earlier work [30]. This moment splits into a spin magnetic moment of $\mu_{\text{spin}}(\text{Fe}) = 0.70 \mu_{\text{B}}$ and an orbital magnetic moment of $\mu_{\text{orb}}(\text{Fe}) = 0.03 \mu_{\text{B}}$. Obviously, this is in good agreement with experimental neutron diffraction data of pure BaFe_2As_2 being $0.87 \mu_{\text{B}}$ [8].

If the finite size of the atomic core is ignored, as usually done, the fully relativistic approach described in Ref. [45] splits B_{hf} into five contributions. There are two contributions due to the s electrons that are conventionally ascribed to the Fermi contact interaction. The larger part is the core polarization contribution B_s^c that was demonstrated in numerous studies to be proportional to the local spin magnetic moment μ_{spin} [46–48]. In addition, there is a s -electron contribution from the valence band B_s^v that is due to the polarization and also dominantly due to the population mechanism [49]. For systems with low symmetry there may be a spin dipolar contribution to B_{hf} for the non- s electrons [45,50]. Apart from $p_{1/2}$ states, states with higher angular momentum such as p and d states have zero probability density at the core and for that reason do not contribute to B_{hf} via the Fermi contact term. If spin-orbit coupling is accounted for, as done here, there is an additional contribution due to the spin-orbit induced orbital magnetization [45,50]. As the orbital contribution is in general dominating compared to the spin-dipolar one [45], we use in the following the term orbital for the total field connected with non- s electrons. Thus, for a transition metal, the remaining three contributions are the orbital field B_{ns}^c of the non- s core states and the orbital fields B_p^v and B_d^v of the valence electrons with p and d character, respectively. One arrives for

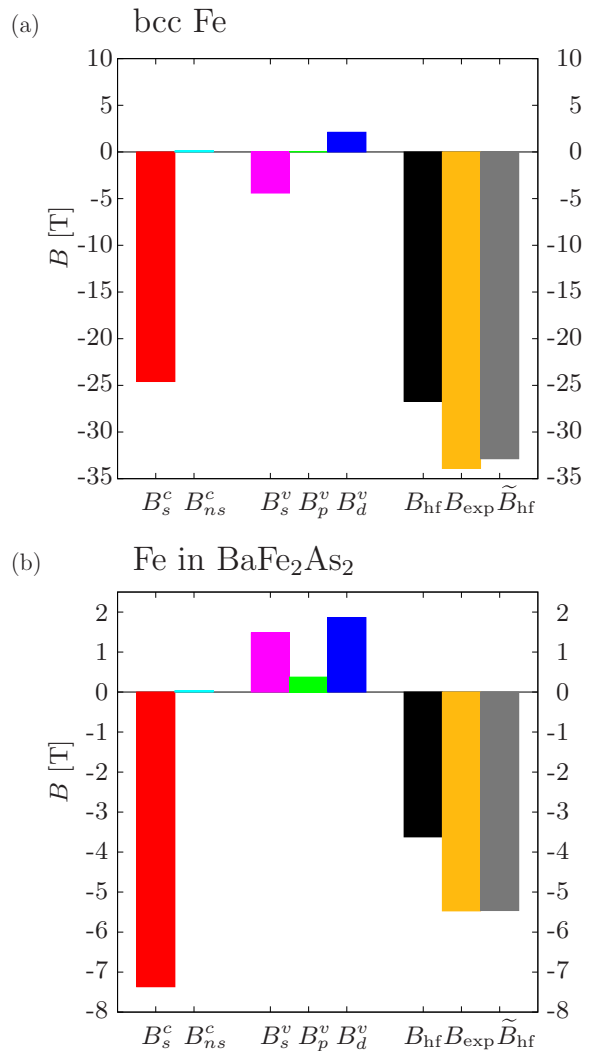


FIG. 1. Contributions to the hyperfine field B_{hf} for (a) bcc Fe and for (b) Fe in antiferromagnetic BaFe_2As_2 . For comparison, experimental values are shown as B_{exp} [9,10,51]. \tilde{B}_{hf} is based on Eq. (2) and includes an enhancement of the core polarization B_s^c of 25%.

the hyperfine field B_{hf} at the following decomposition [45]:

$$B_{\text{hf}} = B_s^c + B_{ns}^c + B_s^v + B_p^v + B_d^v. \quad (1)$$

Figure 1(a) shows for bcc Fe numerical results for the various contributions to the hyperfine field. As it is well known, B_{hf} of bcc Fe is dominated by its large core polarization contribution B_s^c . This is enhanced by the field B_s^v , which is also negative. All other contributions are much smaller and positive. Comparing the total calculated hyperfine field $B_{\text{hf}} = -26.7$ T with the corresponding experimental value $B_{\text{exp}} = -33.9$ T, one finds the theoretical values too small by about 25% [52]. This well known problem is primarily to be ascribed to shortcomings of LSDA when dealing with the core polarization caused by the spin polarization of the valence electrons [53–55]. To cure this problem it is common to enhance B_s^c by about 25% [53–56]. Using this empirical approach one has for the enhanced hyperfine field \tilde{B}_{hf} the

TABLE I. Different contributions to the hyperfine field B_{hf} for BaFe₂As₂, depending on the magnetization direction. Consistent with experiment is an orientation of magnetic moments along the a axis, which was applied throughout this work.

Axis	$\mu_{\text{spin}} (\mu_B)$	B_s^c (T)	B_{ns}^c (T)	B_s^v (T)	B_p^v (T)	B_d^v (T)	B_{hf} (T)
a	0.696	-7.37	0.035	1.48	0.37	1.86	-3.62
b	0.698	-7.39	0.036	1.48	-0.34	2.66	-3.55
c	0.695	-7.36	0.035	1.48	-0.10	-0.13	-6.08

relation

$$\tilde{B}_{\text{hf}} = 1.25 B_s^c + B_{ns}^c + B_s^v + B_p^v + B_d^v. \quad (2)$$

As can be seen in Fig. 1(a), this leads to $\tilde{B}_{\text{hf}} = -32.9$ T for bcc Fe, in good agreement with experiment. Next, consider Fe in the undoped mother compound BaFe₂As₂ as presented in Fig. 1(b). Comparing the calculated $B_{\text{hf}} = -3.62$ T with the experimental one $B_{\text{exp}} = -5.47$ T [9,10], the shortcomings of LSDA are obviously the same as for bcc Fe, as one would expect. However, the enhanced field $\tilde{B}_{\text{hf}} = -5.46$ T is in perfect agreement with experiment, confirming the transferability of the enhancement factor in Eq. (2). Compared with bcc Fe, the various contributions to \tilde{B}_{hf} of Fe in BaFe₂As₂ show two major differences. First, the sign of the valence band s -electron contribution B_s^v is different, and, second, the spin-orbit induced contribution of d electrons B_d^v is considerably higher in the latter case. Both features lead to a very different relation between the enhanced hyperfine field \tilde{B}_{hf} and the local spin magnetic moment μ_{spin} for the two systems. As \tilde{B}_{hf} of bcc Fe is dominated by its enhanced core polarization contribution \tilde{B}_s^c ($\tilde{B}_{\text{hf}}/\tilde{B}_s^c \approx 1.07$), which is proportional to μ_{spin} , it seems justified to assume that the experimental field B_{exp} reflects in a one-to-one manner the local spin moment. For Fe in BaFe₂As₂, on the other hand, we find $\tilde{B}_{\text{hf}}/\tilde{B}_s^c \approx 0.59$, i.e., the total field \tilde{B}_{hf} can by no means be used to monitor the local spin magnetic moment of Fe.

It was found that this unexpected behavior of BaFe₂As₂ compared to bcc Fe is mainly due to its in-plane orientation of magnetic moments along the a axis. It was already stressed that this magnetization direction is conform with experiment [20] and can be theoretically described by the applied inclusion of spin-orbit coupling. For comparison, we show in Table I the components of the hyperfine field of BaFe₂As₂ depending on the magnetization direction. It is obvious that the contributions B_p^v and B_d^v depend strongly on the chosen orientation, although the spin magnetic moment of Fe μ_{spin} and the other contributions to the hyperfine field only marginally change. This has naturally an impact on the total hyperfine field B_{hf} which thus depends on the magnetization direction in BaFe₂As₂.

B. Electron and hole doping

Having investigated the hyperfine field contributions of the undoped BaFe₂As₂ including relativistic effects, an interesting issue is their variation under different types of substitution in the BaFe₂As₂ family.

Two examples of electron doping were investigated, namely, Ba(Fe_{1-x}Co_x)₂As₂ (Co-122) and Ba(Fe_{1-x}Ni_x)₂As₂

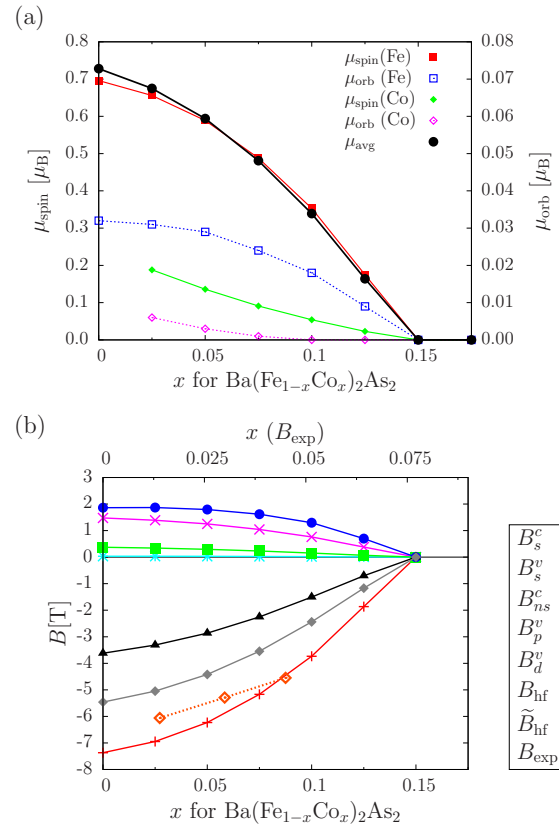


FIG. 2. (a) Component-resolved magnetic moments for Co-122 depending on the concentration x . The left (right) scale refers to the spin (orbital) magnetic moment. (b) Corresponding hyperfine field contributions for Fe in Co-122. The experimental data B_{exp} (dashed orange lines) [24] refer to the upper axis, with the upper and lower axes for the concentration x chosen such that $x_{\text{crit}} = x_{\text{crit,exp}}$.

(Ni-122), with the corresponding data shown in Figs. 2 and 3, respectively. Furthermore, one case of hole doping, (Ba_{1-x}K_x)Fe₂As₂ (K-122), has been considered (see Fig. 4). In all cases, the magnetic moments of the components are presented in Figs. 2(a), 3(a), and 4(a), respectively, as a function of the concentration. The magnetic moments for Co-122 in Fig. 2(a) were published before [30], and are reproduced here to supply a reference for the hyperfine field and to allow for direct comparison with other systems. The various figures give in a component-resolved manner the spin magnetic moments μ_{spin} (left axis) and the orbital magnetic moments μ_{orb} (right axis). The concentration dependent average of the system with composition Ba(Fe_{1-x}TM_x)₂As₂ is shown as $\mu_{\text{avg}} = (1-x)[\mu_{\text{spin}}(\text{Fe}) + \mu_{\text{orb}}(\text{Fe})] + x[\mu_{\text{spin}}(\text{TM}) + \mu_{\text{orb}}(\text{TM})]$.

First consider the electron doped compounds Co-122 and Ni-122. Both systems show a similar decrease in μ_{avg} until the breakdown of long range antiferromagnetic (AFM) order at x_{crit} is reached, with $x_{\text{crit}}(\text{Co-122}) = 0.125$ and $x_{\text{crit}}(\text{Ni-122}) = 0.075$, respectively. This is in reasonable agreement with experiment, with the experimental $x_{\text{crit,exp}}$ being lower [$x_{\text{crit,exp}}(\text{Co-122}) \approx 0.075$ [57], $x_{\text{crit,exp}}(\text{Ni-122}) \approx 0.0375$ [58]]. Concerning the instability of the antiferromagnetic order, the electronic structure calculations account for a change in the nesting condition due to a shift of the Fermi level

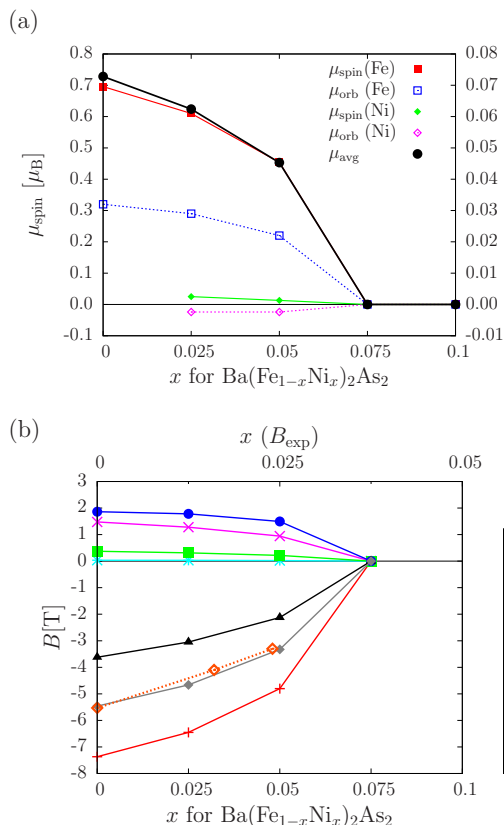


FIG. 3. Same as for Fig. 2, but for Ni-122 with experimental data from Ref. [25].

due to doping but they do not explicitly account for fluctuating magnetic moments or incommensurate spin-density waves [59]. This might explain the observed discrepancies between x_{crit} and $x_{\text{crit,exp}}$, implying that these aspects should be accounted for in order to get better agreement.

In line with experiment, x_{crit} for Ni-122 is found to be only half of Co-122. This had to be expected because of the formal doubling of electron doping by Ni compared to Co substitution of Fe. Another difference between these two compounds is the lower Ni moment in Ni-122 compared to that of Co in Co-122. In this context one should also note that the rather small orbital moment of Ni has a different sign compared to its spin moment. The various hyperfine field contributions for Fe in Co-122 and Ni-122 are shown in Figs. 2(b) and 3(b), respectively. The trends of the Fe magnetic moments and in the hyperfine field contributions behave in a similar way. The figures show also experimental data for the hyperfine field B_{exp} [24,25]. These has been plotted using a different scale for the concentration x at the top of the figure that was chosen such that theoretical and experimental critical concentrations agree ($x_{\text{crit}} = x_{\text{crit,exp}}$). With the aforementioned enhancement of the core polarization field by 25% and the rescaling of the x axis, one finds a very satisfying agreement for \tilde{B}_{hf} and B_{exp} for Co-122 [Fig. 2(b)] as well as Ni-122 [Fig. 3(b)].

Next, the K-122 compound is discussed with its magnetic moments shown in Fig. 4(a) (see also Ref. [60]). A breakdown of the AFM order is found from the calculations at $x_{\text{crit}}(\text{K-122}) = 0.35$, while a lower $x_{\text{crit,exp}}(\text{K-122}) \approx 0.25$

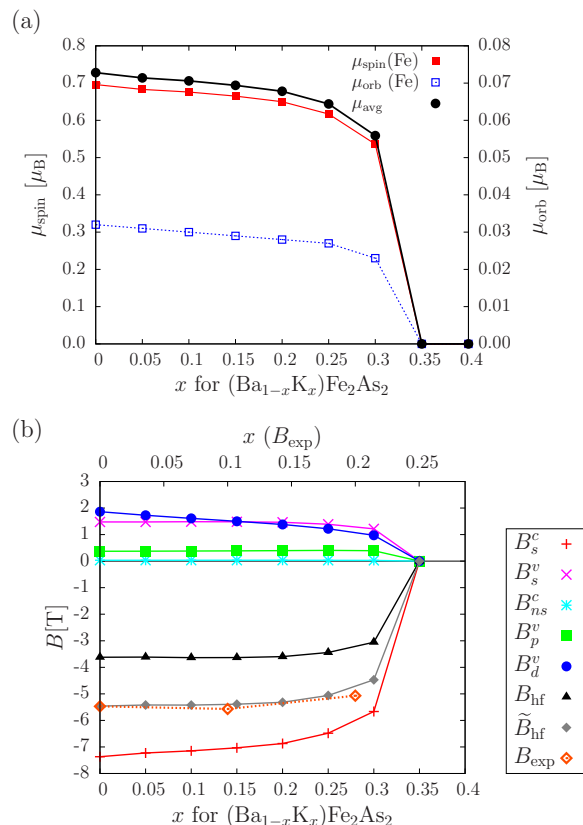


FIG. 4. Same as for Fig. 2, but for K-122 with experimental data from Ref. [10].

[40] is observed in experiment. It should be noted that the substituted K does not have a noteworthy magnetic moment. As the Fe concentration does not change with substitution on the Ba position, the average moment is therefore equal to the Fe moment, leading in this case to $\mu_{\text{avg}} = \mu(\text{Fe}) = \mu_{\text{spin}}(\text{Fe}) + \mu_{\text{orb}}(\text{Fe})$. One can see that for K-122 the magnetic moments change only marginally over a wide concentration range x and undergo a sharp drop for $x > 0.25$. The same behavior can be seen in the hyperfine field contributions of K-122, as shown in Fig. 4(b). Experimental data for B_{exp} [10], referring again to the upper axis, are in good agreement with the enhanced theoretical field \tilde{B}_{hf} . In particular, the experimental B_{exp} is also nearly constant over a large range of concentration, in variance to the electron doped systems considered above.

C. Isovalent doping

The subsequently discussed $\text{Ba}(\text{Fe}_{1-x}\text{Ru}_x)_2\text{As}_2$ (Ru-122) and $\text{BaFe}_2(\text{As}_{1-x}\text{P}_x)_2$ (P-122) compounds are fundamentally different from the systems considered above because of the isovalent doping. This means, in particular, that the VCA is inappropriate to deal with these systems in a meaningful way. Still, a supercell approach could be applied to deal with the substitution [61]. However, the large computational effort makes theoretical work on these compounds rare and difficult. On the other hand, CPA-based approaches provide an efficient and powerful framework for this task.

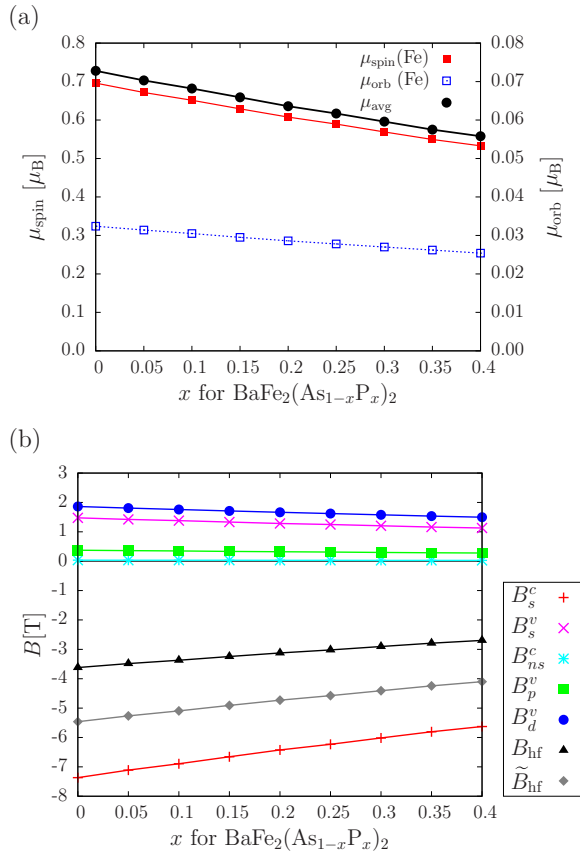


FIG. 5. Same as for Fig. 2, but for P-122.

We show the component-resolved magnetic moments of P-122 and Ru-122 in Figs. 5(a) and 6(a), respectively. The first point to note is that the calculations do not lead to a critical concentration x_{crit} within the investigated regime of substitution, while on the experimental side one has $x_{\text{crit,exp}}(\text{Ru-122}) \approx x_{\text{crit,exp}}(\text{P-122}) \approx 0.3$ [62,63]. Isovalent doping should in general shift the Fermi level E_F only marginally, leading to an unchanged nesting behavior. Thus, magnetic ordering may be preserved as long as the substitutional limit $x \rightarrow 1$ has a finite magnetic moment. In the case of electron or hole doping of BaFe_2As_2 the breakdown of magnetic order at a critical concentration x_{crit} can be understood solely by the nesting condition when the Fermi energy E_F changes due to substitution. Note that also K-122 shows a finite x_{crit} with good agreement to experiment, although the substitution happens not on the Fe position but within the Ba layer. On the other hand, isovalent substitution either within (Ru-122) or outside (P-122) the Fe layer cannot explain the magnetic breakdown by the substitution alone. This indicates that other phenomena not accounted for within the CPA mean field approach influence the stability of the magnetic structure. In the literature, e.g., magnetic dilution was discussed as the main driving force for the magnetic breakdown in Ru-122 [64,65]. Although we find a decrease in the magnetic moments due to the decrease in the Fe content, it seems not sufficient to cause a breakdown of the magnetic order without further reasons. Spin fluctuations and incommensurate spin-density waves can have an impact on the stability of the antiferromagnetic order, but also the

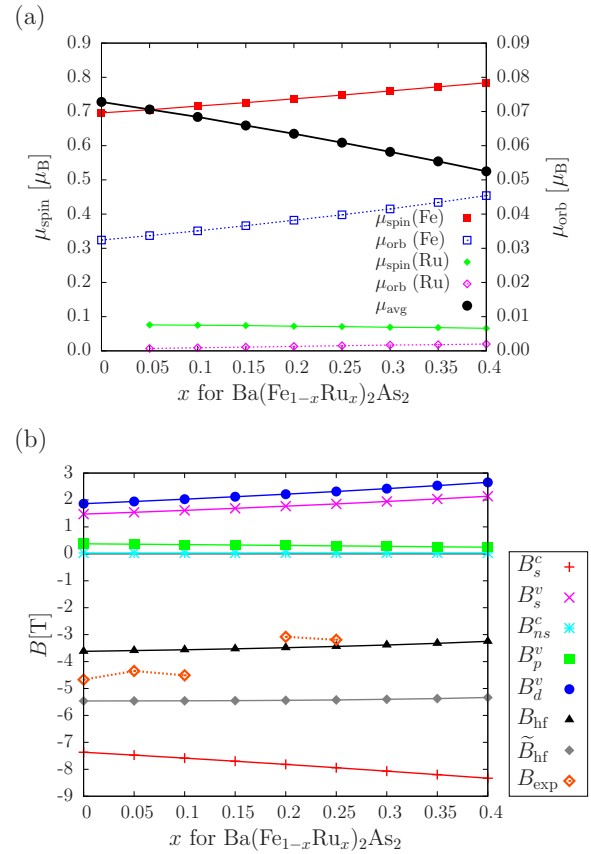


FIG. 6. Same as for Fig. 2, but for Ru-122 with experimental data from Ref. [26].

emergence of a competing superconducting state might play a role. In any case, it becomes obvious that the isovalently doped compounds of the BaFe_2As_2 family are even more difficult to understand than the electron and hole doped variants. Nevertheless, LSDA-based calculations can reproduce the decrease of the average magnetic moment μ_{avg} for Ru-122 as well as for P-122, although the details of this reduction in the magnetic moments are fundamentally different.

The magnetic moments and the hyperfine field contributions of Fe in P-122 shown in Fig. 5 behave in a similar way as those of K-122 (Fig. 4). In both cases the substitution takes place outside the Fe layer; i.e., although the Fe concentration does not change the total Fe moment, $\mu(\text{Fe})$ does. The hyperfine field contributions of Fe in P-122 vary again similar with composition as the magnetic moments do. Of course, this has to be expected as the hyperfine field reflects the magnetization of the Fe atoms, which are the only magnetic components of these systems.

For Ru-122 the average moment μ_{avg} shown in Fig. 6(a) decreases due to the increasing concentration of Ru which has a small induced magnetic moment of around $\mu(\text{Ru}) \approx 0.07\mu_B$, independent on the concentration x . However, the local Fe spin magnetic moment $\mu_{\text{spin}}(\text{Fe})$ and orbital $\mu_{\text{orb}}(\text{Fe})$ magnetic moments surprisingly increase. This is a rather unexpected finding as it was not observed so far within theoretical investigations on the iron pnictides. Accordingly, the corresponding relation to the directly measurable hyperfine

field B_{hf} of Fe is of interest as it provides an element specific probe of the magnetic properties. As can be seen in Fig. 6(b), B_{hf} stays more or less constant over the whole investigated regime of substitution, although $\mu(\text{Fe})$ increases. This is due to the fact that $\mu_{\text{spin}}(\text{Fe})$ and $\mu_{\text{orb}}(\text{Fe})$ simultaneously increase, leading to a subsequent increase of the absolute values of B_s^c and B_d^y . Because the sign of both contributions is different, their changes essentially compensate each other. This does not contradict with experimental findings of Reddy *et al.* [26] depicted in Fig. 6(b) which show a more or less constant B_{hf} for Ru concentrations $x \leq 0.1$. The rapid drop to lower B_{hf} values for Ru-122 for $x \geq 0.2$ is most likely connected to the proximity to the critical concentration x_{crit} , which could not be reproduced by our LSDA-based calculations.

In conclusion, a quite unexpected and interesting variation of the magnetic moments and the hyperfine field with the concentration x of the Ru-122 compound was found which is consistent with experimental findings. This shows, in particular, that Ru-122 and P-122 differ more from each other with respect to their magnetic properties, as one might expect for two isovalently doped pnictides.

D. Relation to the magnetic moment

Finally, the results can be used to clarify the relation between B_{hf} and the average magnetic moment μ_{avg} . It is quite common to assume that the ratio $A_{\text{hf}}^{\text{avg}} = -B_{\text{hf}}/\mu_{\text{avg}}$ or $A_{\text{hf}} = -B_{\text{hf}}/\mu_{\text{spin}}(\text{Fe})$ is constant and use this value in order to obtain the magnetic moments in related compounds from the Fe hyperfine fields. For example, $A_{\text{hf}}^{\text{avg}}(\text{Fe}) = 15 \text{ T}/\mu_{\text{B}}$ was given for bulk Fe and $A_{\text{hf}}^{\text{avg}}(\text{Fe}^{3+}) = 11 \text{ T}/\mu_{\text{B}}$ for Fe^{3+} ions in Fe_2O_3 [25]. These values give for BaFe_2As_2 with an experimental hyperfine field $B_{\text{exp}} = -5.47 \text{ T}$ a magnetic moment $\mu_{\text{avg}} \sim 0.4\text{--}0.5 \mu_{\text{B}}$ [9,10]. Later on it was questioned whether these ratios $A_{\text{hf}}^{\text{avg}}$ are applicable to the iron pnictides [24,25]. In addition, there is general work showing that a scaling of B_{hf} with the corresponding magnetic moment μ_{avg} cannot be assumed *a priori* because $A_{\text{hf}}^{\text{avg}}$ varies strongly for different materials [51]. This is in line with our results that can be used to quantify $A_{\text{hf}}^{\text{avg}}$. Additionally, the assumption of a constant ratio $A_{\text{hf}}^{\text{avg}}$ for doped systems can be disproved, supporting other work [24] which concludes that B_{hf} is indeed not proportional to μ_{avg} for BaFe_2As_2 -based substitutional systems.

As stressed already, the core s -electron contribution B_s^c is indeed proportional to $\mu_{\text{spin}}(\text{Fe})$, which is quantified for our calculations in Fig. 7(a), where we show the ratio $A_c = -B_s^c/\mu_{\text{spin}}(\text{Fe})$ for all investigated compounds depending on the concentration x . Independent on x , we find the value of A_c is nearly constant, $10.6 \text{ T}/\mu_{\text{B}}$. This is in reasonable agreement with earlier work of Lindgren and Sjøström where a value around $12.6 \text{ T}/\mu_{\text{B}}$ was calculated [48]. However, B_s^c can obviously vary significantly from B_{hf} , as was extensively shown in the literature.

At least for the undoped BaFe_2As_2 , the average moment equals the total Fe moment and is close to the spin magnetic moment of iron, $\mu_{\text{avg}} = \mu_{\text{spin}}(\text{Fe}) + \mu_{\text{orb}}(\text{Fe}) \approx \mu_{\text{spin}}(\text{Fe})$. Based on the calculations, one gets for BaFe_2As_2 a ratio $A_{\text{hf}} = -B_{\text{hf}}/\mu_{\text{spin}}(\text{Fe}) = 5.2 \text{ T}/\mu_{\text{B}}$, or based on the enhanced hyperfine field \tilde{B}_{hf} , a ratio $\tilde{A}_{\text{hf}} = 7.8 \text{ T}/\mu_{\text{B}}$. This

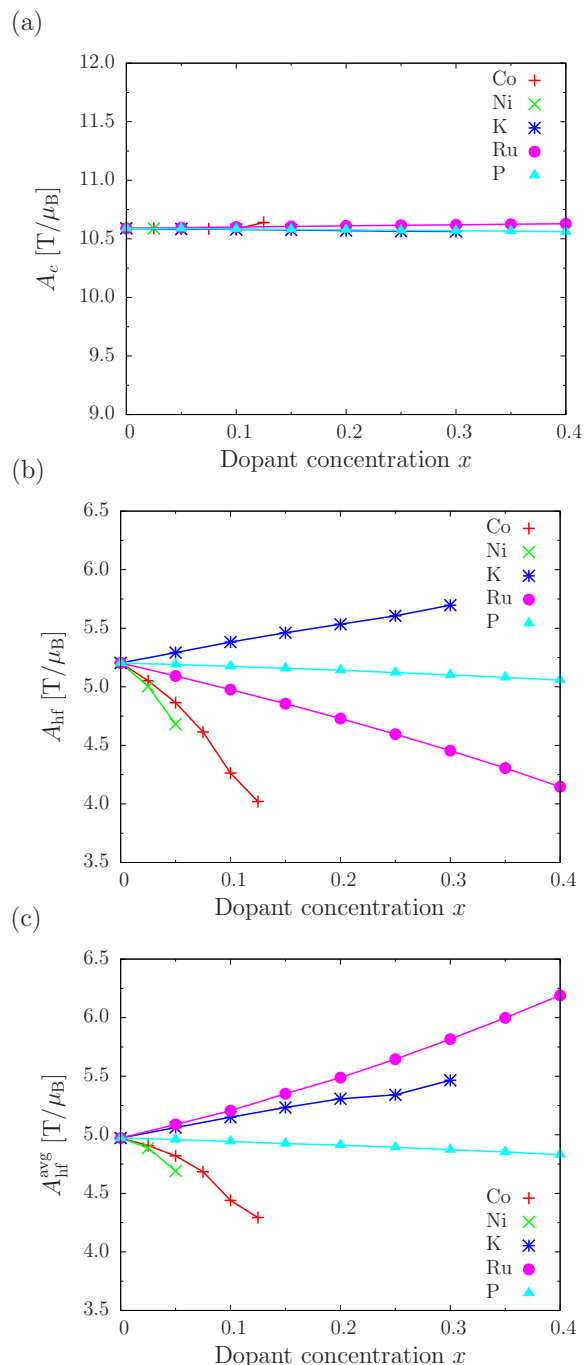


FIG. 7. (a) The ratio $A_c = -B_s^c/\mu_{\text{spin}}(\text{Fe})$ is shown for all investigated compounds, depending on the respective dopant and its concentration x . The constant behavior shows a reasonable relation to the magnetic moment μ . However, the same ratios are shown for (b) $A_{\text{hf}} = -B_{\text{hf}}/\mu_{\text{spin}}(\text{Fe})$ and for (c) $A_{\text{hf}}^{\text{avg}} = -B_{\text{hf}}/\mu_{\text{avg}}$, having huge deviations for a constant A_{hf} behavior, depending on x and on the chosen dopant.

is by a factor of 2–3 different from the ratio $A_{\text{hf}}^{\text{avg}}(\text{Fe})$ applied in previous publications [9,10]. Consequently, the magnetic moment of BaFe_2As_2 based on the measured hyperfine field of 5.47 T should be not between $0.4 \mu_{\text{B}}$ and $0.5 \mu_{\text{B}}$ but rather in the range between $0.7 \mu_{\text{B}}$ and $1.0 \mu_{\text{B}}$, which is in better qualitative agreement with neutron diffraction, reporting

0.87 μ_B [8]. Nevertheless, one should keep in mind that this is a qualitative estimation and it is clear from the literature [24,51] and from our work that an estimation of μ_{avg} based on B_{hf} should be avoided as far as possible.

However, for the doped iron pnictides there is a significant difference between μ_{avg} and $\mu_{\text{spin}}(\text{Fe})$. Thus, the relation between B_{hf} and μ_{avg} leads to an unpredictable, nonlinear behavior of the ratio $A_{\text{hf}}^{\text{avg}}$. To quantify our claim we plot the obtained values of $A_{\text{hf}} = -B_{\text{hf}}/\mu_{\text{spin}}(\text{Fe})$ and $A_{\text{hf}}^{\text{avg}} = -B_{\text{hf}}/\mu_{\text{avg}}$ depending on the concentration x for all investigated compounds in Figs. 7(b) and 7(c), respectively. Already the ratio A_{hf} , which is coupled to the spin magnetic moment of Fe, depends strongly on the respective dopant and on the concentration x . It becomes apparent that for such a behavior no reasonable relation between B_{hf} and $\mu_{\text{spin}}(\text{Fe})$ is possible. This problem becomes even more obvious when considering $A_{\text{hf}}^{\text{avg}}$. Here, the Ru-122 compound is interesting to mention because A_{hf} decreases with x while $A_{\text{hf}}^{\text{avg}}$ increases with the concentration. This is due to the fact that the Fe moment in Ru-122 increases while the average moment decreases (see also Fig. 6). Thus, it can be crucially misleading to relate B_{hf} to the average magnetic moment μ_{avg} in doped iron pnictides. Consequently, the presented study clearly shows that the hyperfine fields B_{hf} of Fe obtained from ⁵⁷Fe Mössbauer spectroscopy are not suitable to make predictions about the respective magnetic moment μ_{avg} in doped iron pnictide superconductors for different substitutions.

IV. SUMMARY

To summarize, this work presented a comprehensive theoretical study of the hyperfine fields in the iron pnictide superconductor family of BaFe₂As₂ with good agreement with experiment. The CPA was applied to a variety of

compounds, dealing accurately with the substitutional disorder and accounting for all variants of doping. This includes electron doped Ba(Fe_{1-x}Co_x)₂As₂ and Ba(Fe_{1-x}Ni_x)₂As₂, hole doped (Ba_{1-x}K_x)Fe₂As₂, and also isovalently doped Ba(Fe_{1-x}Ru_x)₂As₂ and BaFe₂(As_{1-x}P_x)₂. All systems were investigated in their antiferromagnetic state which was used to study the magnetic moments depending on the concentration x in detail. In order to get meaningful results the fully relativistic Dirac formalism was applied, which ensured that all relativistic contributions to B_{hf} were accurately dealt with. Indeed, spin-orbit induced contributions were found to have a significantly higher influence on Fe in BaFe₂As₂, as found for bulk Fe. In particular, the orientation of magnetic moments along the a axis, consistent with experiment, plays a significant role for the hyperfine field. Consequently, we have quantified in detail why it is not sensible to apply the bulk Fe ratio $A_{\text{hf}}^{\text{avg}}(\text{Fe}) = 15 \text{ T}/\mu_B$ to the iron pnictides in order to obtain estimations for the magnetic moment from ⁵⁷Fe Mössbauer spectroscopy. As a crude estimate, one might rather expect for undoped BaFe₂As₂ ratios around 5.0–7.5 T/ μ_B , leading to a magnetic moment of roughly 0.7–1.0 μ_B , which is more consistent with neutron diffraction reporting 0.87 μ_B [8]. However, it is best to avoid such estimations, as was shown for the substituted iron pnictide systems. Here, the behavior of $A_{\text{hf}}^{\text{avg}}$ with the concentration x is clearly unpredictable and might lead to wrong conclusions. Thus, relating the hyperfine fields B_{hf} of Fe obtained via ⁵⁷Fe Mössbauer spectroscopy with the magnetic moments should be avoided for substituted iron pnictides.

ACKNOWLEDGMENT

We acknowledge financial support from the DFG Project FOR 1346. J.M. acknowledges project CENTEM PLUS (LO1402) and VEDPMNF (CZ.02.1.01/15.003/358) of Czech ministerium MSMT.

-
- [1] Y. Kamihara, T. Watanabe, M. Hirano, and H. Hosono, *J. Am. Chem. Soc.* **130**, 3296 (2008).
- [2] H. Takahashi, K. Igawa, K. Arii, Y. Kamihara, M. Hirano, and H. Hosono, *Nature (London)* **453**, 376 (2008).
- [3] D. J. Singh, *Phys. Rev. B* **78**, 094511 (2008).
- [4] I. I. Mazin, D. J. Singh, M. D. Johannes, and M. H. Du, *Phys. Rev. Lett.* **101**, 057003 (2008).
- [5] R. M. Fernandes, D. K. Pratt, W. Tian, J. Zarestky, A. Kreyssig, S. Nandi, M. G. Kim, A. Thaler, N. Ni, P. C. Canfield, R. J. McQueeney, J. Schmalian, and A. I. Goldman, *Phys. Rev. B* **81**, 140501 (2010).
- [6] I. I. Mazin and M. D. Johannes, *Nat. Phys.* **5**, 141 (2009).
- [7] I. I. Mazin, M. D. Johannes, L. Boeri, K. Koepernik, and D. J. Singh, *Phys. Rev. B* **78**, 085104 (2008).
- [8] Q. Huang, Y. Qiu, W. Bao, M. A. Green, J. W. Lynn, Y. C. Gasparovic, T. Wu, G. Wu, and X. H. Chen, *Phys. Rev. Lett.* **101**, 257003 (2008).
- [9] M. Rotter, M. Tegel, D. Johrendt, I. Schellenberg, W. Hermes, and R. Pöttgen, *Phys. Rev. B* **78**, 020503 (2008).
- [10] M. Rotter, M. Tegel, I. Schellenberg, F. M. Schappacher, R. Pöttgen, J. Deisenhofer, A. Günther, F. Schrettle, A. Loidl, and D. Johrendt, *New J. Phys.* **11**, 025014 (2009).
- [11] A. N. Yaresko, G.-Q. Liu, V. N. Antonov, and O. K. Andersen, *Phys. Rev. B* **79**, 144421 (2009).
- [12] I. Opahle, H. C. Kandpal, Y. Zhang, C. Gros, and R. Valentí, *Phys. Rev. B* **79**, 024509 (2009).
- [13] J. Fink, S. Thirupathaiah, R. Ovsyannikov, H. A. Dürr, R. Follath, Y. Huang, S. de Jong, M. S. Golden, Y.-Z. Zhang, H. O. Jeschke, R. Valentí, C. Felser, S. Dastjani Farahani, M. Rotter, and D. Johrendt, *Phys. Rev. B* **79**, 155118 (2009).
- [14] M. J. Han, Q. Yin, W. E. Pickett, and S. Y. Savrasov, *Phys. Rev. Lett.* **102**, 107003 (2009).
- [15] L. X. Yang, Y. Zhang, H. W. Ou, J. F. Zhao, D. W. Shen, B. Zhou, J. Wei, F. Chen, M. Xu, C. He, Y. Chen, Z. D. Wang, X. F. Wang, T. Wu, G. Wu, X. H. Chen, M. Arita, K. Shimada, M. Taniguchi, Z. Y. Lu, T. Xiang, and D. L. Feng, *Phys. Rev. Lett.* **102**, 107002 (2009).
- [16] L. Craco, M. S. Laad, S. Leoni, and H. Rosner, *Phys. Rev. B* **78**, 134511 (2008).
- [17] D. Kasinathan, A. Ormeci, K. Koch, U. Burkhardt, W. Schnelle, A. Leithe-Jasper, and H. Rosner, *New J. Phys.* **11**, 025023 (2009).
- [18] A. Sanna, F. Bernardini, G. Profeta, S. Sharma, J. K. Dewhurst, A. Lucarelli, L. Degiorgi, E. K. U. Gross, and S. Massidda, *Phys. Rev. B* **83**, 054502 (2011).

- [19] E. Aktürk and S. Ciraci, *Phys. Rev. B* **79**, 184523 (2009).
- [20] Y. Su, P. Link, A. Schneidewind, T. Wolf, P. Adelman, Y. Xiao, M. Meven, R. Mittal, M. Rotter, D. Johrendt, T. Brueckel, and M. Loewenhaupt, *Phys. Rev. B* **79**, 064504 (2009).
- [21] H. Gretarsson, A. Lupascu, J. Kim, D. Casa, T. Gog, W. Wu, S. R. Julian, Z. J. Xu, J. S. Wen, G. D. Gu, R. H. Yuan, Z. G. Chen, N.-L. Wang, S. Khim, K. H. Kim, M. Ishikado, I. Jarrige, S. Shamoto, J.-H. Chu, I. R. Fisher, and Y.-J. Kim, *Phys. Rev. B* **84**, 100509 (2011).
- [22] P. Vilmercati, A. Fedorov, F. Bondino, F. Offi, G. Panaccione, P. Lacovig, L. Simonelli, M. A. McGuire, A. S. M. Sefat, D. Mandrus, B. C. Sales, T. Egami, W. Ku, and N. Mannella, *Phys. Rev. B* **85**, 220503 (2012).
- [23] S. V. Borisenko, D. V. Evtushinsky, Z.-H. Liu, I. Morozov, R. Kappenberger, S. Wurmehl, B. Büchner, A. N. Yaresko, T. K. Kim, M. Hoesch, T. Wolf, and N. D. Zhigadlo, *Nat. Phys.* **12**, 311 (2016).
- [24] P. Bonville, F. Rullier-Albenque, D. Colson, and A. Forget, *Europhys. Lett.* **89**, 67008 (2010).
- [25] I. Nowik, I. Felner, N. Ni, S. L. Bud'ko, and P. C. Canfield, *J. Phys.: Condens. Matter* **22**, 355701 (2010).
- [26] V. R. Reddy, A. Bharathi, A. Gupta, K. Sharma, S. Chandra, S. Sharma, K. Vinod, and C. S. Sundar, *J. Phys.: Condens. Matter* **26**, 356002 (2014).
- [27] J. M. Allred, K. M. Taddei, D. E. Bugaris, M. J. Krogstad, S. H. Lapidus, D. Y. Chung, H. Claus, M. G. Kanatzidis, D. E. Brown, J. Kang, R. M. Fernandes, I. Eremin, S. Rosenkranz, O. Chmaissem, and R. Osborn, *Nat. Phys.* **12**, 493 (2016).
- [28] H. Pang, Y. Fang, and F. Li, *Hyperfine Interact.* **199**, 387 (2011).
- [29] G. Derondeau, S. Polesya, S. Mankovsky, H. Ebert, and J. Minár, *Phys. Rev. B* **90**, 184509 (2014).
- [30] G. Derondeau, J. Braun, H. Ebert, and J. Minár, *Phys. Rev. B* **93**, 144513 (2016).
- [31] G. Derondeau, F. Bisti, J. Braun, V. A. Rogalev, M. Kobayashi, M. Shi, T. Schmitt, J. Ma, H. Ding, H. Ebert, V. N. Strocov, and J. Minár, *arXiv:1606.08977*.
- [32] T. Berlijn, C.-H. Lin, W. Garber, and W. Ku, *Phys. Rev. Lett.* **108**, 207003 (2012).
- [33] S. N. Khan and D. D. Johnson, *Phys. Rev. Lett.* **112**, 156401 (2014).
- [34] S. N. Khan, A. Alam, and D. D. Johnson, *Phys. Rev. B* **89**, 205121 (2014).
- [35] A. Herbig, R. Heid, and J. Schmalian, *Phys. Rev. B* **94**, 094512 (2016).
- [36] H. Ebert, D. Ködderitzsch, and J. Minár, *Rep. Prog. Phys.* **74**, 096501 (2011).
- [37] H. Ebert *et al.*, *The Munich SPR-KKR Package*, version 6.3, <http://olymp.cup.uni-muenchen.de/ak/ebert/SPRKKR>, 2012.
- [38] L. Vegard, *Z. Phys.* **5**, 17 (1921).
- [39] A. S. Sefat, R. Jin, M. A. McGuire, B. C. Sales, D. J. Singh, and D. Mandrus, *Phys. Rev. Lett.* **101**, 117004 (2008).
- [40] M. Rotter, M. Pangerl, M. Tegel, and D. Johrendt, *Angew. Chem. Int. Ed.* **47**, 7949 (2008).
- [41] A. Thaler, N. Ni, A. Kracher, J. Q. Yan, S. L. Bud'ko, and P. C. Canfield, *Phys. Rev. B* **82**, 014534 (2010).
- [42] M. Rotter, Ph.D. thesis, LMU München, 2010.
- [43] M. Merz, P. Schweiss, P. Nagel, M.-J. Huang, R. Eder, T. Wolf, H. von Löhneysen, and S. Schuppler, *J. Phys. Soc. Jpn.* **85**, 044707 (2016).
- [44] S. H. Vosko, L. Wilk, and M. Nusair, *Can. J. Phys.* **58**, 1200 (1980).
- [45] M. Battoletti and H. Ebert, *Phys. Rev. B* **64**, 094417 (2001).
- [46] H. Akai, M. Akai, S. Blügel, R. Zeller, and P. H. Dederichs, *J. Magn. Magn. Mater.* **45**, 291 (1984).
- [47] M. E. Elzain, D. E. Ellis, and D. Guenzburger, *Phys. Rev. B* **34**, 1430 (1986).
- [48] B. Lindgren and J. Sjöström, *J. Phys. F: Met. Phys.* **18**, 1563 (1988).
- [49] H. Ebert, H. Winter, D. D. Johnson, and F. J. Pinski, *Hyperfine Interact.* **51**, 925 (1989).
- [50] G. Y. Guo and H. Ebert, *Phys. Rev. B* **53**, 2492 (1996).
- [51] S. Dubiel, *J. Alloys Compd.* **488**, 18 (2009).
- [52] H. Akai and T. Kotani, *Hyperfine Interact.* **120**, 3 (1999).
- [53] S. Blügel, H. Akai, R. Zeller, and P. H. Dederichs, *Phys. Rev. B* **35**, 3271 (1987).
- [54] H. Ebert, P. Strange, and B. L. Gyorffy, *J. Phys. (Paris)* **49**, 31 (1988).
- [55] D. Benea, O. Isnard, J. Minár, H. Ebert, and V. Pop, *J. Appl. Phys.* **109**, 083909 (2011).
- [56] H. Ebert and H. Akai, *Hyperfine Interact.* **78**, 361 (1993).
- [57] C. Lester, J.-H. Chu, J. G. Analytis, S. C. Capelli, A. S. Erickson, C. L. Condon, M. F. Toney, I. R. Fisher, and S. M. Hayden, *Phys. Rev. B* **79**, 144523 (2009).
- [58] N. Ni, A. Thaler, J. Q. Yan, A. Kracher, E. Colombier, S. L. Bud'ko, P. C. Canfield, and S. T. Hannahs, *Phys. Rev. B* **82**, 024519 (2010).
- [59] D. K. Pratt, M. G. Kim, A. Kreyssig, Y. B. Lee, G. S. Tucker, A. Thaler, W. Tian, J. L. Zarestky, S. L. Bud'ko, P. C. Canfield, B. N. Harmon, A. I. Goldman, and R. J. McQueeney, *Phys. Rev. Lett.* **106**, 257001 (2011).
- [60] G. Derondeau, J. Minár, S. Wimmer, and H. Ebert, *arXiv:1608.08077*.
- [61] L. Wang, T. Berlijn, Y. Wang, C.-H. Lin, P. J. Hirschfeld, and W. Ku, *Phys. Rev. Lett.* **110**, 037001 (2013).
- [62] M. G. Kim, D. K. Pratt, G. E. Rustan, W. Tian, J. L. Zarestky, A. Thaler, S. L. Bud'ko, P. C. Canfield, R. J. McQueeney, A. Kreyssig, and A. I. Goldman, *Phys. Rev. B* **83**, 054514 (2011).
- [63] D. Hu, X. Lu, W. Zhang, H. Luo, S. Li, P. Wang, G. Chen, F. Han, S. R. Banjara, A. Sapkota, A. Kreyssig, A. I. Goldman, Z. Yamani, C. Niedermayer, M. Skoulatos, R. Georgii, T. Keller, P. Wang, W. Yu, and P. Dai, *Phys. Rev. Lett.* **114**, 157002 (2015).
- [64] R. S. Dhaka, C. Liu, R. M. Fernandes, R. Jiang, C. P. Strehlow, T. Kondo, A. Thaler, J. Schmalian, S. L. Bud'ko, P. C. Canfield, and A. Kaminski, *Phys. Rev. Lett.* **107**, 267002 (2011).
- [65] R. S. Dhaka, S. E. Hahn, E. Razzoli, R. Jiang, M. Shi, B. N. Harmon, A. Thaler, S. L. Bud'ko, P. C. Canfield, and A. Kaminski, *Phys. Rev. Lett.* **110**, 067002 (2013).